Synthesis of High Aspect Ratio Low-Silica Zeolite L Rods in Oil/Water/Surfactant Mixtures

C. Shane Carr and Daniel F. Shantz*

Department of Chemical Engineering, Texas A&M University, 3122 TAMU, College Station, Texas 77843-3122

Received August 10, 2005. Revised Manuscript Received September 21, 2005

Low-silica zeolite L (zeolite GL) syntheses in the presence of emulsions were investigated. High aspect ratio rods were obtained when zeolite LTL was crystallized in the presence of both cationic and nonionic two-phase emulsions. Conventional syntheses of zeolite L primarily led to low aspect ratio crystals possessing a length/width ratio of approximately 1.5. In the presence of the emulsion aspect ratios were increased with most samples possessing aspect ratios between 5 and 10, although crystals were observed with aspect ratios as high as 42. TEM analysis indicates the LTL pores are parallel to the long axis of the crystals. It is observed that anisotropic crystals are formed when the surfactant (CTAB) to cation ratio is below 3.5. By contrast when the CTAB/($Ba^{2+}+K^{+}$) is greater than four the LTL phase does not form. Igepal CO-720 was also used to determine if similar high aspect ratio crystals could be formed in nonionic emulsions. While the nonionic emulsions also led to LTL rods, the phase purity of the materials was lower based on SEM and PXRD. This report, to the best of knowledge, is the first of low-silica zeolite L crystals (Si/Al < 1.5) that possess such aspect ratios. Given the ability to exchange at least some of the extraframework cations, the materials reported here are possible candidates for use in applications including microelectronics and sensing.

Introduction

Zeolite L (LTL) is a commercially important zeolite that has been studied because of its ion exchange capabilities and unusually high thermal stability as compared to other low-silica zeolites. Zeolite L was first synthesized by Breck in the 1960s using a potassium-based synthesis procedure.[1] Since that initial work, numerous investigations have explored the synthesis, characterization, and application of LTL materials. Many works have reported incorporating metal clusters into zeolite L, most notably platinum,[2−18] although other metals such as iridium,[19−21] gallium,[22] and iron[23] have been introduced. Using zeolite L nanocrystals as seeds for growing zeolite thin films has also been investigated.[24] Also of relevance to the current work, typically zeolite L is formed possessing a Si/Al between 3 and 6; it is possible to make low-silica LTL phases, even with a Si/Al = 1. Such materials were originally reported by Barrer and Mainwairing[25,26] and were denoted as GL zeolites. Typically these materials are made in barium-rich mixtures.[27]

Given the potential of zeolite L in catalysis and that the catalytic properties of zeolites are often strongly related to the particle size and morphology, controlling the size and shape of zeolite L crystals is of interest. Tsapatsis et al.

* To whom correspondence should be addressed. Phone: (979) 845-3492. Fax: (979) 845-6446. E-mail: Shantz@che.tamu.edu.

(1) Breck, D.; Acara, N. U.S. Patent 3216789, 1965.
(2) Besoukhanova, C.; Guidot, J.; Barthomeuf, D.; Breysse, M.; Bernard, J. R. *J. Chem. Soc.-Faraday Trans. I* **1981**, *77*, 1595−1604.
(3) Larsen, G.; Haller, G. L. *Catal. Lett.* **1989**, *3*, 103−110.
(4) Vaarkamp, M.; Grondelle, J. V.; Miller, J. T.; Sajkowski, D. J.; Modica, F. S.; Lane, G. S.; Gates, B. C.; Koningsberger, D. C. *Catal. Lett.* **1990**, *6*, 369−382.
(5) Davis, R. J.; Derouane, E. G. *Nature* **1991**, *349*, 313−315.
(6) Lane, G. S.; Modica, F. S.; Miller, J. T. *J. Catal.* **1991**, *129*, 145−158.
(7) Hong, S. B.; Mielczarski, E.; Davis, M. E. *J. Catal.* **1992**, *134*, 349−358.
(8) Larsen, G.; Haller, G. L. *Catal. Today* **1992**, *15*, 431−442.
(9) Mielczarski, E.; Hong, S. B.; Davis, R. J.; Davis, M. E. *J. Catal.* **1992**, *134*, 359−369.
(10) Han, W. J.; Kooh, A. B.; Hicks, R. F. *Catal. Lett.* **1993**, *18*, 219−225.
(11) Iglesia, E.; Baumgartner, J. E.; Haller, G.; Paal, Z.; Barthomeut, D.; Ponec, V.; Sachtler, W. M. H.; Figueras, F. *Stud. Surf. Sci. Catal.* **1993**, *75*, 993−1006.
(12) McVicker, G. B.; Kao, J. L.; Ziemiak, J. J.; Gates, W. E.; Robbins, J. L.; Treacy, M. M. J.; Rice, S. B.; Vanderspurt, T. H.; Cross, V. R.; Ghosh, A. K. *J. Catal.* **1993**, *139*, 48−61.
(13) Davis, R. J. *Heterogeneous Chem. Rev.* **1994**, *1*, 41−53.
(14) Cho, S. J.; Ahn, W. S.; Hong, S. B.; Ryoo, R. *J. Phys. Chem.* **1996**, *100*, 4996−5003.
(15) Jacobs, G.; Padro, C. L.; Resasco, D. E. *J. Catal.* **1998**, *179*, 43−55.
(16) Jentoft, R. E.; Tsapatsis, M.; Davis, M. E.; Gates, B. C. *J. Catal.* **1998**, *179*, 565−580.
(17) Jacobs, G.; Ghadiali, F.; Pisanu, A.; Borgna, A.; Alvarez, W. E.; Resasco, D. E. *Appl. Catal., A* **1999**, *188*, 79−98.
(18) Enderle, B. A.; Labouriau, A.; Ott, K. C.; Gates, B. C. *Nano Lett.* **2002**, *2*, 1269−1271.
(19) Triantafillou, N. D.; Miller, J. T.; Gates, B. C. *J. Catal.* **1995**, *155*, 131−140.
(20) Triantafillou, N. D.; Deutsch, S. E.; Alexeev, O.; Miller, J. T.; Gates, B. C. *J. Catal.* **1996**, *159*, 14−22.
(21) Zhao, A. L.; Jentoft, R. E.; Gates, B. C. *J. Catal.* **1997**, *169*, 263−274.
(22) Newsam, J. M. *Mater. Res. Bull.* **1986**, *21*, 661−672.
(23) Ko, Y. S.; Ahn, W. S.; Chae, J. H.; Moon, S. H. Synthesis and characterization of iron modified L-type zeolite. In *Progress in Zeolite and Microporous Materials, Pts A−C*; Elsevier Science B.V.: New York, 1997; pp 733−740.
(24) Lovallo, M. C.; Tsapatsis, M.; Okubo, T. *Chem. Mater.* **1996**, *8*, 1579−1583.
(25) Barrer, R. M.; Beaumont, R.; Collela, C. *J. Chem. Soc., Dalton* **1974**, 934−941.
(26) Barrer, R. M.; Mainwaring, D. E. *J. Chem. Soc., Dalton* **1972**, 1259−1265.
(27) Barrer, R. M.; Sieber, W. *J. Chem. Soc., Dalton* **1978**, 598−601.

10.1021/cm051790k CCC: $30.25
Published on Web 10/28/2005

reported the synthesis of nanocrystals of zeolite L of approximately 40 nm in length with aspect ratios between 2 and 3.[28] More recently, works have been published on growing micrometer-sized LTL crystals of controllable morphology. Larlus et al.[29] reported varying reaction conditions and material stoichiometry to achieve a variety of crystal morphologies and sizes. Large crystals were made ranging from 2 to 5 μm, although in most cases the aspect ratios appear to be less than 2 for these materials. Lee et al.[30] have also examined changing reaction conditions to achieve flat-faceted zeolite L crystals with enhanced aspect ratios. Crystals were reported between 2 and 20 μm in length with aspect ratios that ranged from 2 to 30. Both of these studies used high-temperature syntheses that ranged from 150 to 200 °C in the work by Larlus et al.[29] and 180 °C in the work by Lee et al.[30] Reported Si/Al ratios in these works are typically between 4 and 6. Also, Calzaferri's lab has reported on the synthesis of zeolite L nanocrystals and their use as device components.[31−33] To the best of our knowledge, however, morphological control of low-silica LTL crystals has not been reported. This is of great interest, given that low-silica LTL crystals typically have pores that run along the axis of the crystal and a high density of extraframework cations. The ability to selectively control the aspect ratio of LTL crystals would allow for the generation of containers that could function as hosts for nanowires growth, enabling the use of such materials in a variety of applications including sensing, ion conduction, thermoelectrics, etc.

The work reported here explores another approach to manipulating crystal morphology. Microemulsions (thermodynamically stable one-phase mixtures consisting of surfactant, oil, and water) have recently drawn interest as a means to controlling zeolite crystal growth.[34−47] Studies in our lab have looked at the effect of microemulsions on both low-silica[48] and high-silica zeolite formation.[40,41,47] Our work demonstrates that microemulsion-mediated syntheses result in zeolitic crystals with unique morphologies and microstructures as compared to conventional syntheses. Our initial work in low-silica zeolites focused on zeolite A,[48] given the wealth of previous literature for comparison. In that work it proved difficult to grow crystals with anisotropic morphologies. This is likely due to the fact zeolite A possesses cubic symmetry, and one would expect no inherent differences in the growth energetics along different crystal directions. In that regard LTL is a more interesting choice given it possesses hexagonal symmetry.

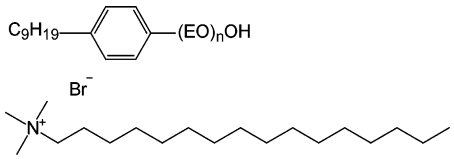

Figure 1. Structures of (top) Igepal CO-720 and (bottom) cetyltrimethylammonium bromide.

In this study, low-silica LTL (GL) crystals are grown in two-phase oil/water/ surfactant/cosurfactant mixtures (i.e., emulsions, primarily a cetyltrimethylammonium−heptane−butanol−zeolite system) at 368 K. This allows for direct determination of the phase behavior under actual synthesis conditions. This study examines three issues: (1) determination of the crystal morphology obtainable from syntheses employing emulsions, (2) assessment of how different emulsion properties (i.e., composition) impact the growth of the material, and (3) comparison to conventional syntheses.

Experimental Section

Zeolite Synthesis. The surfactants used in this work were cetyltrimethylammonium bromide (CTAB, Sigma-Aldrich, >99%) and Igepal CO-720 (n = 12, Sigma-Aldrich, >99%) (Figure 1). Heptane (EMD, >98%), isooctane (Mallinckrodt, 99%), and butanol (EMD, >99%) were used as received. The zeolite reagents used were kaolin (Sigma-Aldrich, USP grade), which was converted to metakaolin via calcination at 923 K, barium hydroxide octahydrate (Sigma-Aldrich, >98%), potassium hydroxide (VWR, 45% w/w in water), and water. The synthesis used was the same as that reported by Burton and Lobo (1:4.46:0.245:292 $SiAlO_{7/2}$:KOH:Ba$(OH)_2$:H_2O),[49] with the only difference being the synthesis temperature, 368 K in this work versus 358 K in their report. A typical synthesis mixture was prepared as follows: 2.13 g of 45 wt % KOH solution and 0.3 g of $Ba(OH)_2 \cdot 8H_2O$ were dissolved in 19.04 g of H_2O in an autoclavable Teflon container. To this mixture, 0.43 g of metakaolinite was added and stirred at room temperature for 10 min.

The emulsions consist of the surfactant, oil (heptane), water, and cosurfactant (butanol). The surfactant:butanol weight ratio is 2:1 for all samples unless noted otherwise. Synthesis mixtures will be denoted below as oil:surfactant/cosurfactant:zeolite (weight fractions). The emulsion synthesis involves premixing of the oil, surfactant, and butanol in a borosilicate glass test tube to allow for as much dissolution as possible. To this mixture, appropriate amounts of the zeolite mixture were added. As a representative example, 2 g of CTAB were mixed with 4 g of heptane and 1 g of butanol for 30 min, followed by the addition of 3 g of zeolite mixture. This is represented as 0.4:0.3:0.3 oil:(CTAB + butanol):

(28) Tsapatsis, M.; Lovallo, M.; Okubo, T.; Davis, M. E.; Sadakata, M. *Chem. Mater.* **1995**, *7*, 1734−1741.
(29) Larlus, O.; Valtchev, V. P. *Chem. Mater.* **2004**, *16*, 3381−3389.
(30) Lee, Y. J.; Lee, J. S.; Yoon, K. B. *Microporous Mesoporous Mater.* **2005**, *80*, 237−246.
(31) Huber, S.; Calzaferri, G. *Angew. Chem., Int. Ed.* **2004**, *43*, 6738−6742.
(32) Megelski, S.; Calzaferri, G. *Adv. Funct. Mater.* **2001**, *11*, 277−286.
(33) Zabala, A.; Bruwhiler, D.; Ban, T.; Calzaferri, G. *Monatsh. Chem.* **2005**, *136*, 77−89.
(34) Dutta, P. K.; Castagnola, M. J. *Microporous Mesoporous Mater.* **1998**, *20*, 149−159.
(35) Dutta, P. K.; Jakupca, M.; Reddy, K. S. N.; Salvati, L. *Nature* **1995**, *374*, 44−46.
(36) Dutta, P. K.; Robins, D. *Langmuir* **1991**, *7*, 1048−1050.
(37) Singh, R.; Doolittle, J., J.; George, M. A.; Dutta, P. K. *Langmuir* **2002**, *18*, 8193−8197.
(38) Singh, R.; Dutta, P. K. *Langmuir* **2000**, *16*, 4148−4153.
(39) Reddy, K. S. N.; Salvati, L. M.; Dutta, P. K.; Abel, P. B.; Suh, K. I.; Ansari, R. R. *J. Phys. Chem.* **1996**, *100*, 9870−9880.
(40) Lee, S.; Shantz, D. F. *Chem. Commun.* **2004**, 680−681.
(41) Lee, S.; Shantz, D. F. *Chem. Mater.* **2005**, *17*, 409−417.
(42) Lin, J.-C.; Dipre, J. T.; Yates, M. Z. *Chem. Mater.* **2003**, *15*, 2764−2773.
(43) Lin, J.-C.; Dipre, J. T.; Yates, M. Z. *Langmuir* **2004**, *20*, 1039−1042.
(44) Lin, J.-C.; Yates, M. Z. *Langmuir* **2005**, *21*, 2117−2120.
(45) Manna, A.; Kulkarni, B. D.; Ahedi, R. K.; Bhaumik, A.; Kotasthane, A. N. *J. Colloid Interface Sci.* **1999**, *213*, 405−411.
(46) Yates, M. Z.; Ott, K. C.; Birnbaum, E. R.; McCleskey, T. M. *Angew. Chem., Int. Ed.* **2002**, *41*, 476−478.
(47) Axnanda, S.; Shantz, D. F. *Microporous Mesoporous Mater.* **2005**, *84*, 236−246.
(48) Carr, C. S.; Shantz, D. F. *Microporous Mesoporous Mater.* **2005**, *85*, 284−292.
(49) Burton, A.; Lobo, R. F. *Microporous Mesoporous Mater.* **1999**, *33*, 97−113.

Table 1. Summary of LTL Samples Made in CTAB Emulsions; S/C Is the CTAB/ (Ba^{2+} + K^+) Ratio

sample ID	H:S:Z	length (nm)	diameter (nm)	aspect ratio (L/D)	S/C (mol/mol)
CTAB-A	0.6:0.2:0.2	930	130	7.1	2.2
CTAB-B	0.5:0.3:0.2	850	110	7.7	3.3
CTAB-C	0.4:0.4:0.2				4.4
CTAB-D	0.5:0.2:0.3	710	150	4.7	1.5
CTAB-E	0.4:0.3:0.3	2500	60	41.7	2.2
CTAB-F	0.35:0.35:0.3	950	140	6.8	2.6
CTAB-G	0.35:0.25:0.4	1000	110	9.1	1.4
CTAB-H	0.35:0.15:0.5	800	80	7.0	0.7
CTAB-I	0.25:0.25:0.5	910	170	5.3	1.1
CTAB-J	0.25:0.35:0.4	1200	120	10	1.9
control	0:0:1	260	200	1.3	

zeolite. The tests tubes were typically 50−75% full. After 10 min of mixing, the test tubes were sealed with a screw cap and placed in an oven under quiescent conditions at 368 K for 4 days unless noted. Samples were recovered by filtration and washed with copious amounts of deionized water and ethanol.

Characterization. Powder X-ray diffraction (PXRD) was performed on a Bruker D-8 X-ray diffractometer with Cu Kα radiation. Samples were analyzed over a range of 2−40° 2θ using a step size of 0.05° and a step rate of 2 s/step. Field-emission scanning electron microscopy (FE-SEM) measurements were performed using a Zeiss Leo-1530 microscope operating at 1−10 kV. Transmission electron microscopy (TEM) was performed on a JEOL 2010 microscope with a lanthanum hexaboride filament and an excitation voltage of 200 kV. The samples were mortared and pestled, then dispersed in ethanol (100%, Aldrich), and placed on a 400-mesh copper grid. Energy dispersive X-ray analysis (EDX) was performed using an Oxford instrument eXL EDS system. One-pulse ^{29}Si MAS NMR measurements were performed on a Bruker Avance spectrometer operating at 79.48 MHz. Spectra were acquired using a 4 mm probe with ZrO_2 rotors, a spinning rate of 5 kHz, a 2 μs 45° pulse, high-power proton decoupling, and a 20 s recycle delay. Chemical shifts are referenced to tetramethylsilane.

Results

Cationic Emulsions: Effect of the Emulsion on Zeolite Formation/Growth. Initial work explored the use of CTAB−butanol−heptane−water (zeolite) mixtures. Axnanda and Shantz reported the phase diagram of this system without zeolite at 368 K,[47] and the one-phase region is in the low water content portion of the diagram. All syntheses in this work were performed in the two-phase region of the phase diagram as determined by visual inspection. Syntheses performed in the one-phase region yielded amorphous materials based on PXRD. This is most likely due to the high surfactant concentration needed to form the one-phase mixture. Tago et al.[50] reported that the CTA^+ and TPA^+ ions compete in the formation of MFI when both are present. It is expected that a similar effect exists in this synthesis with barium and potassium ions competing with the CTA^+ cations, which explains why increased CTAB concentrations suppress zeolite formation.

The samples made in CTAB-based emulsions are summarized in Table 1. These materials were compared to a zeolite L sample made under the same reaction conditions without the emulsion. Figure 2 shows the PXRD patterns of LTL samples made without the emulsion and for one of the samples made in the emulsion. No major differences are apparent in the PXRD patterns. Both samples in Figure 2 are zeolite L, indicating that at these conditions the emulsion does not result in inhibition of zeolite growth or the appearance of impurities. Figure 3 shows the ^{29}Si MAS spectrum of the sample made in the emulsion shown in Figure 2. There are two lines in the spectrum, one at −88.5 ppm and another at −91.4 ppm. The line at −88.5 ppm is consistent with results reported by Burton and Lobo for GL materials.[49] The line at −91.4 is the (Si3Al) resonance. Based on this assumption, integration of the ^{29}Si spectrum gives a Si/Al = 1.15 ± 0.05. This is consistent with EDX analysis of the sample in three locations that gives an average value of 1.35 ± 0.02. Given that NMR is a "bulk" sampling method, this value seems more reliable. In any event, the crystals formed clearly have a Si/Al < 1.5.

The FE-SEM images of the conventional synthesis product and the sample made in the emulsion are shown in Figure 4. The crystals made in the absence of the emulsion are cylinders approximately 200−500 nm in size with diameters of approximately 100−200 nm. There are a variety of aspect

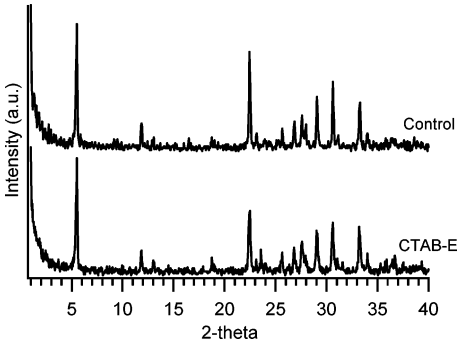

Figure 2. PXRD patterns of LTL samples grown in the (top) absence and (bottom) presence of CTAB emulsions.

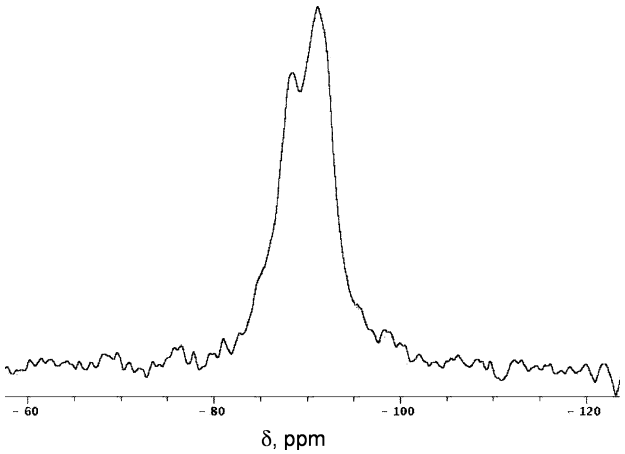

Figure 3. ^{29}Si MAS spectrum of CTAB-E.

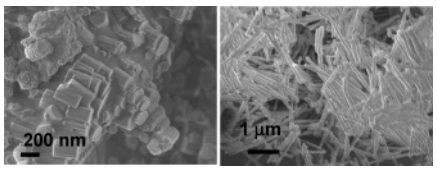

Figure 4. FE-SEM of LTL sample made without the emulsion (left) and in a CTAB emulsion (CTAB-E, right).

(50) Tago, T.; Nishi, M.; Kouno, Y.; Masuda, T. *Chem. Lett.* **2004**, *33*, 1040−1041.

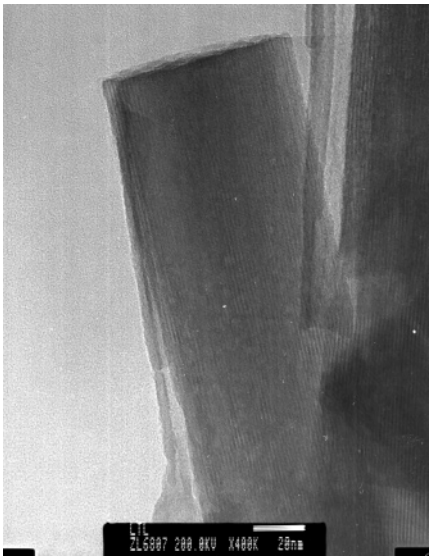

Figure 5. TEM image of LTL crystals made in CTAB emulsions (CTAB-E). Scale bar is 20 nm.

ratios present in this sample ranging from 1 to 6, but the majority of the particles formed have aspect ratios of approximately 1.5. The samples made in the emulsion typically possess much higher aspect (*L/D*) ratios. The sample with the highest aspect ratio is rods approximately 1−3 μm in length and 50−100 nm in diameter. These values were determined from several FE-SEM images for each sample. The diameter of the rods appears quite uniform (±10 nm), while the lengths of the rods possess some polydispersity (ca. ±100 nm). Table 1 summarizes the particle size and aspect ratio as determined by FE-SEM. It is clear that the emulsion has a significant impact on the crystal size and shape. Aspect ratios ranging from 3 to 42 are observed simply by the inclusion of the emulsion. These results indicate that the emulsion suppresses growth along certain crystallographic directions given the dramatic increase in *L/D* for samples made in the presence of the emulsion. Figure 5 shows a TEM image of CTAB-E. From the image it can be observed that the pores are parallel to the long axis of the crystal, as is typically observed for LTL crystals.

Cationic Emulsions: Effect of Emulsion Composition. Syntheses were performed to assess how the emulsion composition affects material properties. The PXRD patterns shown in Figure 6 and the Supporting Information indicate that all of the materials are LTL-type zeolite, with minor impurities present in materials CTAB-C, -F, and -J (these impurities are most likely attributable to OFF-type zeolite). Because all of the materials are crystalline as shown by the PXRD data, microscopy was used to determine any relationship between the emulsion composition and the resulting crystal morphology.

The FE-SEM images for the materials made with CTAB are shown in Figure 7 and the Supporting Information. There are two major morphologies observed in the images: (1) long (>500 nm) rods with large length-to-diameter ratios and (2) smaller cylindrical structures with larger length-to-diameter ratios than the control experiment, but less than the rods. CTAB-C is the only sample that does not possess these morphologies. Interestingly, it is also the sample with

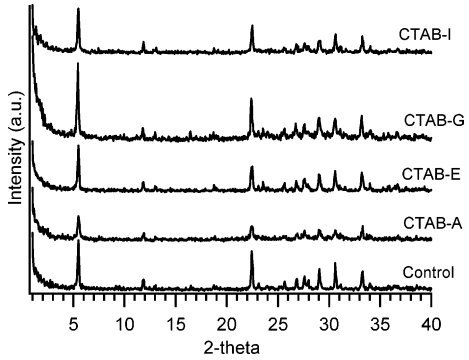

Figure 6. PXRD patterns of LTL samples formed in CTAB emulsions.

Table 2. Summary of LTL Samples Made in Nonionic Emulsions

sample ID	H:S:Z	length (nm)	diameter (nm)	aspect ratio (L/D)	S/C (mol/mol)
720-A	0.2:0.7:0.1	1500	200	7.5	7.6
720-B	0.3:0.6:0.1				6.5
720-C	0.4:0.5:0.1	1200	150	8.0	5.4
720-D	0.1:0.8:0.1	1100	120	9.2	8.6
720-E	0.2:0.6:0.2				3.2

the highest surfactant-to-cation (CTAB/(K^++Ba^{2+})) ratio (S/C = 4.4 see Table 1). That this synthesis did not lead to zeolite L is consistent with the syntheses in the one-phase region also being unsuccessful, given that syntheses in the one-phase region also have high surfactant-to-cation ratios. The PXRD pattern (Supporting Information) also shows a greatly reduced first peak (approximately 5.5° 2θ) and the presence of a peak at 22.5° 2θ that is much larger than that in the control sample, suggesting that other impurities are present. In all cases the aspect ratio determined by FE-SEM is >4 and larger than 7 for several of the samples. The one clear observation that emerges is that high S/C ratios (e.g., CTAB-C) lead to poorly crystalline material. The samples that show the long rodlike structure are CTAB-E, CTAB-G, CTAB-H, and CTAB-J. The sample with the largest aspect ratio is CTAB-E, with lengths of approximately 2−3 μm and diameters of less than 100 nm. The smaller cylindrical particles (CTAB-A, CTAB-B, and CTAB-D) are grown in mixtures with lower zeolite weight fractions (<0.3). CTAB-A and CTAB-B both have relatively high S/C ratios of 2.2 and 3.3 respectively due to the low amount of zeolite present. CTAB-D has a much lower S/C ratio (1.5). Why sample CTAB-E has a much higher aspect ratio than the other syntheses is not clear; however, this result is reproducible as this synthesis was repeated three times with very similar results. More importantly is that all of the syntheses reported above that lead to LTL formation also result in crystals with significantly different aspect ratios (5−10) as compared to the synthesis in the absence of the oil/water/surfactant mixture (~1.5). To elucidate the potential role of surfactant adsorption and surfactant−silicate electrostatic forces in zeolite growth, emulsions formed by other surfactants were studied.

Nonionic Emulsions. Five separate tests were run using Igepal CO-720 as the surfactant and are summarized in Table 2. FE-SEM images (Figure 8) indicate the presence of high aspect ratio crystals and the PXRD patterns are shown in Figure 9. The most obvious thing to note is the absence of

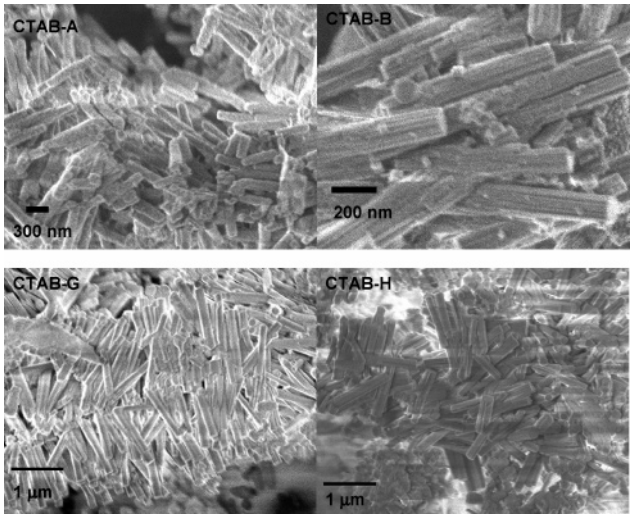

Figure 7. FE-SEM images of LTL grown in CTAB emulsions.

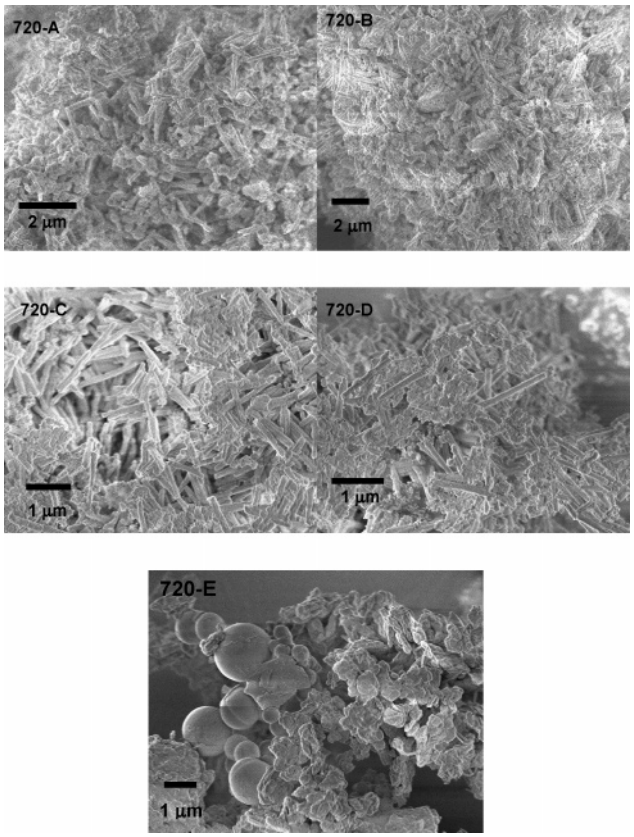

Figure 8. FE-SEM images of LTL samples grown in Igepal CO-720 emulsions.

diffraction peaks for the 720-E sample. In contrast to the ionic emulsion synthesis, here a high surfactant-to-zeolite ratio is desirable. Sample 720-E is the only sample with a 3.2 S/C ratio as the rest of the samples tested are 5.4 or higher. The FE-SEM image (Figure 8) is also consistent with the formation of amorphous material. 720-B is the only sample other than 720-E that does not have obvious rods present (6.5 S/C). Like in CTAB-C, there is a strong peak at around 23.5° 2θ, which indicates that this is not a pure LTL material. 720-C and 720-D are well-defined rods and correspond to S/C ratios of 5.4 and 8.6. The FE-SEM images also show that there is some poorly defined material in these samples, indicating the presence of some impurities.

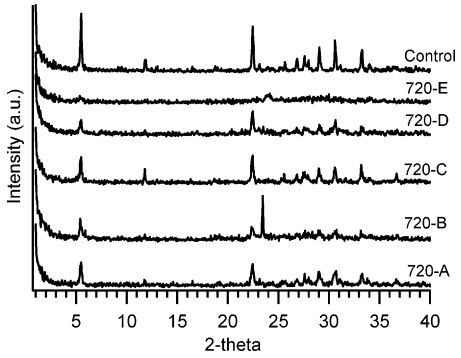

Figure 9. PXRD patterns of LTL samples grown in Igepal CO-720 emulsions.

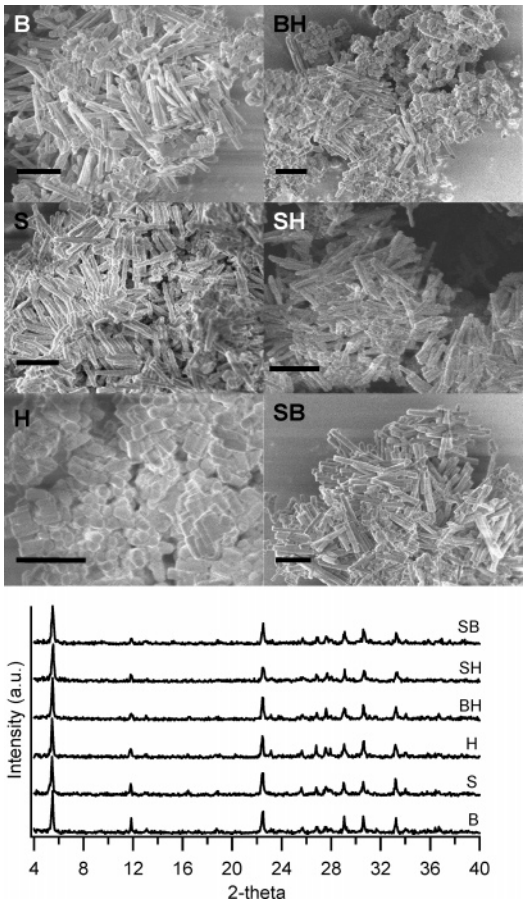

Figure 10. (Top) FE-SEM images of control samples. "B" stands for butanol, "S" for surfactant (CTAB), and "H" for heptane. All scale bars are 1 μm. (Bottom) PXRD patterns of control samples.

Control Experiments. Syntheses were performed where one (or two) of the emulsion components were removed to understand the role of the individual microemulsion components. The PXRD patterns of the samples are shown in Figure 10. Crystals with fairly large aspect ratios are obtainable in many of the samples as seen in the FE-SEM images (Figure 10). The only sample that does not show high aspect ratio crystals is the synthesis using heptane with no surfactant or butanol. The aspect ratios for the CTAB only, CTAB + butanol, and butanol-only syntheses are estimated by FE-SEM to be 8.3, 6.6, and 7.0, respectively. The material with butanol and heptane (no surfactant) shows a mixture of low aspect ratio materials similar to the heptane-only materials and higher aspect ratio materials such as the butanol-only sample. That crystals made only in the presence

of butanol is consistent with the results from the samples made in the nonionic emulsions. The results of the control experiments reported above are in contrast to previous work from our lab.[41,47,48] In all other systems previously studied (silicalite-1 at 368 K, 433 K, LTA at 333 K) all emulsion components are needed to form the desired materials. This would seem to indicate that it is adsorption of the amphiphile on the inorganic surface that is essential to modifying crystal habit (see below).

Discussion

Although the formation of LTL crystals with high aspect ratios is not a new concept, this research shows zeolite growth in the presence of emulsions can be used to control crystal morphology at milder reaction conditions than most conventional routes. Also noteworthy is the ability to fabricate such high aspect ratio crystals with a Si/Al < 1.5. The aspect ratio can be adjusted by varying the emulsion composition (and subsequently the surfactant-to-zeolite ratio), and there appears to be a specific region that allows for very high aspect ratio materials. The location of this region seems to be based on two key issues: (1) The CTAB emulsion should be in the two-phase region to allow for adequate surfactant/oil/zeolite mixing (not likely in the high zeolite loading region as seen with CTAB-D) but to maintain a suitably low surfactant concentration (shown to be too high in the one-phase region), and (2) there is a range of S/C ratios which seem to be better suited for LTL formation, specifically when S/C < 2.3. High ratios of S/C (i.e., >4) seem to suppress zeolite formation.

The nature of the surfactant seems to play an important role in the crystal morphology obtained. Both nonionic and cationic emulsions were capable of growing the rods; however, nonionic emulsions required large surfactant-to-zeolite ratios. The cationic surfactant CTAB was successful at growing long rods at much lower surfactant-to-zeolite ratios. This could be interpreted as a result of the fact that the electrostatic forces between the cationic surfactant and anionic zeolite surface are much stronger than the van der Waals/steric forces in the case of the nonionic emulsions.

The points above would seem to have implications for the mechanism of crystal habit modification. The control experiments seem to indicate that the "nanoreactor" concept of growth is not valid here. This point is in fact consistent with our previous work in this area. In this context it is important to point out that the zeolite synthesis mixture used is a turbid/viscous liquid, and it was observed that upon heating the zeolite mixture appeared to preferentially partition into the bottom phase of the two-phase emulsion and ultimately sediment out. Also, the control experiments would seem to indicate that the surfactant and/or cosurfactant adsorption on the (alumino)silicate surface is what drives the observed crystal morphologies. That nonionic and cationic surfactants lead to this morphology as well as short-chain alcohols (butanol) is consistent with this observation. The limitation on the cationic emulsions appears to be that there is a threshold surfactant/cation ratio above which the zeolite will not form, indicating competitive interactions (adsorption?) between the alkali cations, surfactants, and (alumino)silicate species in solution. As such it appears that the emulsion does not substantially influence zeolite nucleation, and while the control experiments show that rods can be made without all components of the emulsions, the crystal quality and uniformity is improved for samples made in the emulsions as compared to samples made just in butanol, etc. Ongoing work is exploring growth of these materials in polyols and and will be reported elsewhere.

Conclusions

The current work demonstrates the formation of high aspect ratio low-silica LTL crystals at low temperatures via zeolite growth in the presence of an emulsion. The aspect ratio is tunable based on the emulsion composition. Interestingly, LTL rods can be grown in both ionic and nonionic emulsions. Ongoing work is exploring this in more detail as well as the ion exchange properties of these materials and their potential use as components in microdevices.

Acknowledgment. This work was supported by Texas A&M University. The authors also acknowledge the Microscopy and Imaging Center (MIC) at Texas A&M for access to the TEM facilities, Dr. Zhiping Luo for the TEM and EDX measurements, and the Chemistry Department (TAMU) for access to the powder X-ray diffraction instruments. The FE-SEM instrument was supported by the National Science Foundation under Grant No. DBI-0116835. The solid-state NMR spectrometer was supported by the National Science Foundation under Grant CHE-0234931.

Supporting Information Available: PXRD and FE-SEM images of samples made in CTAB emulsions. This material is available free of charge via the Internet at http://pubs.acs.org.

CM051790K